Macromolecular Materials and Engineering
www.mme-journal.de

Desalination of Seawater Using Cationic Poly(acrylamide) Hydrogels and Mechanical Forces for Separation

*Christian Fengler, Lukas Arens, Harald Horn, and Manfred Wilhelm**

In this study, the ability of cationic poly(acrylamide-*co*-(3-acrylamidopropyl) trimethylammonium chloride) hydrogels to desalinate seawater is explored, where the salt separation is based on the partial rejection of mobile salt ions by the fixed charges along the polymer backbone. Water absorbency measurements reveal that artificial seawater-containing divalent ions (Mg^{2+}, Ca^{2+}, and SO_4^{2-}) drastically decrease the swelling capacity of previously employed anionic poly(acrylic acid-*co*-sodium acrylate) hydrogels, whereas no influence on the swelling behavior of the synthesized cationic hydrogels is found. The swelling behavior and mechanical properties are studied by varying the degree of crosslinking and degree of ionization systematically in the range of 1–5 and 25–75 mol%, respectively. Finally, artificial seawater (c_{sea} = 0.171 mol L^{-1}) is desalinated in a custom-built press setup with an estimated efficiency of E_{m^3} = 17.6 kWh m^{-3} by applying an external pressure on the swollen hydrogels.

1. Introduction

Nowadays, one of the major global risks on human health and economic growth is the lack of potable water supply. It is estimated that 80% of the population is exposed to major threats to water security, which is especially pronounced for areas with rapid population growth and low access to freshwater reservoirs.[1] Since only 0.5% of the world's water is available as freshwater source, a potential method to overcome water scarcity is to implement cost-efficient desalination techniques.[2] Currently, the total desalination capacity stands at 95.37 million m³ per day with ≈16 000 operating desalination plants.[3] Historically, thermal desalination processes, such as multistage flash distillation (MSF), have been predominantly used in the 20th century. Thereafter, the production of desalinated water with membrane systems underwent an exponential increase in recent years, outpacing traditional thermal processes. The desalination capacity of reverse osmosis (RO) processes is estimated to 65.5 million m³ per day, accounting currently for 69% of the total desalination capacity.[3]

In the reverse osmosis process, semipermeable membranes are utilized to separate ions from seawater. An external pressure of up to 100 bar is applied on the feed solution to overcome the osmotic pressure and push the water molecules through the dense membranes. The energy demand is low (3–6 kWh m^{-3}), close to the theoretical limit of 0.8 kWh m^{-3}, which is related to the osmotic pressure of seawater.[4,5] However, major disadvantages such as the high investment costs for the membranes and the regular maintenance due to biofouling and clogging, have not yet been resolved and account for up to 15.5% of the total cost per cubic meter fresh water.[6,7] As a potential alternative it was recently proposed that inexpensive and chemically rather simple polyelectrolyte hydrogels (1–2 € kg^{-1}) can be applied as a separation medium for the desalination of salt water.[8,9] These hydrogels, often referred to as superabsorbent polymers, contain charges along the polymer backbone and show a high affinity to water.[10–12] Due to the high swelling capabilities of up to 1000 times their own weight, polyelectrolytes are predominantly utilized in disposable hygiene products, such as diapers.[10] Other sectors that benefit from these properties are agriculture, pharmaceutics, food protection, and construction.[13–16] Moreover, it was shown that the salt dependent swelling behavior of polyelectrolyte hydrogels can be exploited to generate renewable energy from natural salt gradients, e.g., river deltas in an osmotic engine.[17,18]

In the desalination approach however, the charges along the polymer backbone satisfy two purposes that can be related to forward osmosis (FO) techniques, where drawing agents are used to induce a net flow of water through a semipermeable membrane by establishing an osmotic pressure.[19] The polyelectrolyte hydrogels act as both the drawing agent and separation medium at the same time. The fundamental principle of the separation mechanism is based on the Donnan equilibrium that describes the partitioning of mobile ions between the gel phase and the surrounding solution.[20,21] The desalination is realized in a discontinuous three-step process. First, dry polyelectrolyte hydrogel particles are mixed with saline feedwater, then the salt enriched supernatant phase is removed, and

C. Fengler, Dr. L. Arens, Prof. M. Wilhelm
Karlsruhe Institute of Technology (KIT)
Institute for Technical Chemistry and Polymer Chemistry (ITCP)
Engesserstr. 18, Karlsruhe 76131, Germany
E-mail: manfred.wilhelm@kit.edu
Prof. H. Horn
Karlsruhe Institute of Technology (KIT)
Engler-Bunte-Institut
Engler-Bunte-Ring 1, Karlsruhe 76173, Germany
The ORCID identification number(s) for the author(s) of this article can be found under https://doi.org/10.1002/mame.202000383.

© 2020 The Authors. Published by Wiley-VCH GmbH. This is an open access article under the terms of the Creative Commons Attribution License, which permits use, distribution and reproduction in any medium, provided the original work is properly cited.

DOI: 10.1002/mame.202000383

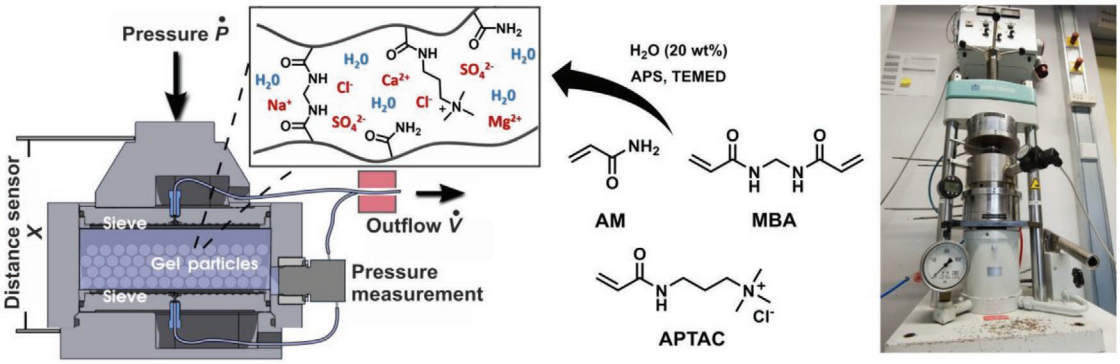

Figure 1. Left: Schematic drawing of the press setup for the desalination of seawater utilizing cationic polyelectrolyte hydrogel particles as a separation medium. Salt depleted water is recovered by deswelling the particles with an external force. The cationic poly(acrylamide-*co*-(3-acrylamidopropyl) trimethylammonium chloride) (PAPTAC) hydrogel particles are synthesized by free radical copolymerization using the respective monomers in water. Right: Technical realization of the press setup.[22] The height of the piston x, elution volume V, and the pressure p are determined with an uncertainty of $\Delta x = 1$ µm, $\Delta V = 0.5$ mL, and $\Delta p = 0.01$ bar. The ion content is measured offline via inductively coupled plasma optical emission spectroscopy (ICP-OES) and ion chromatography.

finally, salt depleted water is recovered by applying an external force on the swollen hydrogel particles using a custom-built press setup, as depicted in **Figure 1**. Applying this desalination approach, potable water from a 35 g L^{-1} (0.171 mol L^{-1}) NaCl solution having similar ionic strength as seawater could be obtained with an estimated energy demand of 8.9 kWh m^{-3}, utilizing highly crosslinked (degree of crosslinking (DC) = 5 mol%) poly(sodium acrylate) hydrogels.[22] In addition, the impact of various network architectures, such as surface crosslinked and interpenetrating hydrogels, on the separation behavior has been investigated.[23] Other studies demonstrated the utilization of temperature (50 °C) instead of pressure as an alternative, renewable stimulus with thermally responsive *N*-isopropylacrylamide hydrogels.[24] Furthermore, analytical thermodynamic models based on the early work of Katchalsky were developed and used to calculate the total energy cost that is required to reduce the salt concentration from 0.6 down to 0.001 mol L^{-1} over multiple swelling–deswelling cycles. The energy demand was estimated to around 1.5–3 kWh m^{-3}.[25]

Previous studies were predominantly aimed on the technical realization and improvement of the desalination efficiency toward salt water by optimizing the hydrogel properties as well as the experimental parameters. Pure sodium chloride solutions were used as a rather simple model system for mimicking seawater which however is a much more complex system, containing multivalent ions, such as Mg^{2+}, Ca^{2+}, and SO_4^{2-}. These multivalent ions can interact with the negatively charged polyelectrolyte backbone and influence the swelling behavior by reducing the swelling capacities of previously employed anionic poly(acrylic acid-*co*-sodium acrylate) (PSA) hydrogels.[26,27] Thus, we propose the use of cationic hydrogels as an alternative separation medium to overcome the aforementioned limit.

The here presented study is organized as follows: first, a series of cationic poly(acrylamide-*co*-(3-acrylamidopropyl) trimethylammonium chloride) (PAPTAC) hydrogels are synthesized by varying the DC and degree of ionization (DI) systematically in the range of 1–5 and 25–75 mol%, respectively. Second, the swelling behavior of the synthesized cationic hydrogel is investigated in different salt solutions ($MgCl_2$, $CaCl_2$, and Na_2SO_4) as well as artificial seawater with concentrations varying from 0.017 to 0.17 mol L^{-1} and compared to an anionic PSA hydrogel (DC = 1 mol%; DI = 75 mol%) that is used as a reference system. In addition, rheological measurements are performed to study the impact of the hydrogel composition on the network formation and mechanical properties. Finally, salt rejection measurements are conducted to investigate the influence of charge density on salt partitioning. As a proof of concept, the most promising sample is used for the desalination of artificial seawater in the press setup which is displayed in Figure 1.

2. Experimental Section

2.1. Materials

(3-Acrylamidopropyl)trimethylammonium chloride (APTAC, 75 wt%, Sigma-Aldrich), acrylamide (AM, 99%, Sigma-Aldrich), *N,N,N′,N′*-tetramethylethylenediamine (TEMED, 99.5%, Acros Organics), ammonium persulfate (APS, >99%, Acros Organics), *N,N′*-methylenebis(acrylamide) (MBA, 99%, Sigma-Aldrich), sodium chloride (NaCl, 99%, Acros Organics), sodium hydroxide (NaOH, 33 wt%, Acros Organics), sodium persulfate (SPS, >98%, Sigma-Aldrich), calcium chloride ($CaCl_2$, 99%, Sigma-Aldrich), sodium sulfate (Na_2SO_4, 99%, Riedel-de Haen), and magnesium chloride hexahydate ($MgCl_2{\cdot}6H_2O$, 98%, Fluka) were used as received. Acrylic acid (AA, >99%, Merck) was freshly distilled at reduced pressure prior to the synthesis.

2.2. Synthesis of Cationic Poly(acrylamide-*co*-(3-acrylamidopropyl)trimethylammonium chloride) Hydrogels

PAPTAC hydrogels were synthesized by free radical polymerization (FRP) of acrylamide (AM) and (3-acrylamidopropyl) trimethylammonium chloride (APTAC) in water with *N,N′*-methylenebis(acrylamide) (MBA) as difunctional crosslinking agent, as displayed in Figure 1. The synthesis procedure was adapted from literature and slightly optimized as follows.[28] First, a 20 wt% solution of monomers (AM, APTAC and MBA) in water was prepared and the polymerization started after the

© 2020 The Authors. Published by Wiley-VCH GmbH

addition of APS and TEMED as radical–redox initiating system. To take into account the amount of 4-methoxyphenol (MEHQ) inhibitor that is present in the APTAC monomer solution, the amount of APS und TEMED was adjusted and calculated according to Equation (1). Samples with a varying degree of crosslinking (DC = 1, 3, and 5 mol%) and degree of ionization (DI = 25, 50, and 75 mol%) were synthesized, which are given by Equations (2) and (3), respectively

$$n(\text{APS, TEMED}) = 0.5\ \text{mol\%} \times n(\text{AM} + \text{APTAC}) + n(\text{MEHQ}) \quad (1)$$

$$\text{DC} = \frac{n(\text{MBA})}{n(\text{AM} + \text{APTAC})} \times 100\ \text{mol\%} \quad (2)$$

$$\text{DI} = \frac{n(\text{APTAC})}{n(\text{AM} + \text{APTAC})} \times 100\ \text{mol\%} \quad (3)$$

The synthesis of the sample with DC = 1 mol% and DI = 25 mol% is here given as an example. First, MBA (0.103 g, 0.667 mmol) was dissolved in deionized water (25.3 g). Subsequently, AM (3.55 g, 0.05 mol) and APTAC (3.45 g, 0.0167 mol) as 75 wt% solution were added. TEMED (0.0516 g, 0.444 mmol) was added and the mixture was cooled with an ice bath and purged with nitrogen for 30 min. Then, APS (0.101 g, 0.444 mmol) was dissolved in deionized water (2 g) and added to the mixture to initiate the polymerization. The gelation typically started within 1 h and was allowed to complete overnight. The hydrogels were cut into small pieces and placed in a large excess of deionized water for 4 days to remove unreacted chemicals and sol content. The purified samples were dried in a vacuum oven at 60 °C for 3 days. The dry particles were grinded and sieved to obtain particles with sizes between 300 and 600 µm. The anionic PSA hydrogel reference system with DI = 75 mol% and DC = 1 mol% was synthesized in a similar fashion, using sodium hydroxide to deprotonate carboxylic acid and generate negative charges in the network. The procedure has been described in previous work in more detail.[17] An overview of the synthesized samples is displayed in **Table 1**.

Table 1. Overview of the synthesized samples.

Sample name	DC [mol%]	DI [mol%]
PAPTAC_DC1_DI25	1	25
PAPTAC_DC1_DI50	1	50
PAPTAC_DC1_DI75	1	75
PAPTAC_DC3_DI25	3	25
PAPTAC_DC3_DI50	3	50
PAPTAC_DC3_DI75	3	75
PAPTAC_DC5_DI25	5	25
PAPTAC_DC5_DI50	5	50
PAPTAC_DC5_DI75	5	75
PSA_DC1_DI75	1	75

The varied synthetic parameters degree of crosslinking (DC) and degree of ionization (DI) are given in columns 2 and 3 while the sample names are derived from these quantities. The abbreviations PAPTAC and PSA refer to the cationic poly(acrylamide-*co*-(3-acrylamidopropyl)trimethylammonium chloride) and anionic PSA hydrogel, respectively.

2.3. Water Absorbency Measurements

The degree of swelling at equilibrium (Q_{eq}) was measured gravimetrically. ≈10 mg of the dried hydrogel sample (m_p) with a particle diameter between 350 and 650 µm was placed on a metal sieve (m_{sieve}) with a mesh size of 120 µm. The sieve was put on a metal rack, which was then placed in a Petri dish filled with the solution to let the particles swell overnight. Then, the sieve with the swollen particles was pressed on a paper towel to remove excess solution and weighed ($m_{swollen}$). The degree of swelling was calculated according to Equation (4)

$$Q_{eq} = \frac{m_{swollen} - m_{sieve} - m_p}{m_p}\ [\text{g g}^{-1}] \quad (4)$$

Hydrogel samples were measured in aqueous sodium chloride solutions with concentrations ranging from 0.017 to 0.71 mol L^{-1}. Artificial seawater containing the most prominent salts (NaCl, $MgCl_2$, Na_2SO_4, and $CaCl_2$) was prepared according to the composition of ASTM international (ASTM D1141) with concentrations similar to the sodium chloride solutions between 0.017 and 0.71 mol L^{-1}.[29] The ratio between the salts was kept constant for various concentrations. Absorbency measurements in pure multivalent salt solutions ($MgCl_2$, Na_2SO_4, and $CaCl_2$) were performed with concentrations ranging from 0.34 to 128 mmol L^{-1}. The reported results are the average of three independent measurements with a standard deviation of $\sigma_Q < 5\%$.

2.4. Rheology and Sample Preparation

Mechanical properties of the hydrogels were analyzed via oscillatory shear experiments on the strain-controlled rheometer ARES G2 (TA Instruments, Eschborn, Germany). Hydrogel samples were prepared in a cylindrical mold with a diameter of 30 mm to obtain uniform disc-shaped specimens with a height of 5 mm. The mold was sealed and the crosslinking reaction was allowed to proceed overnight. The disc-shaped specimens were measured directly without further purification. The test geometry was a 30 mm diameter plate made of aluminum. The geometry was lowered until a constant axial force of 0.5 N (177 Pa) was applied to the sample and the temperature was controlled to 25 ± 0.1 °C by a Peltier element (Advanced Peltier System, TA Instruments). First, an oscillatory strain sweep from γ_0 = 0.01 to 1000% was performed for every sample at a constant frequency of ω = 6.3 rad s^{-1} (f = 1 Hz) by varying the strain to determine the linear viscoelastic (LVE) regime. The values at a strain of γ_0 = 0.1% were chosen to be representative for the LVE regime. Frequency sweeps for three different specimens of the hydrogel sample were conducted at a fixed strain of γ_0 = 0.1% and the frequency was varied from ω = 0.2 to 630 rad s^{-1}. From these experiments the mean value of the elastic (G') and viscous

© 2020 The Authors. Published by Wiley-VCH GmbH

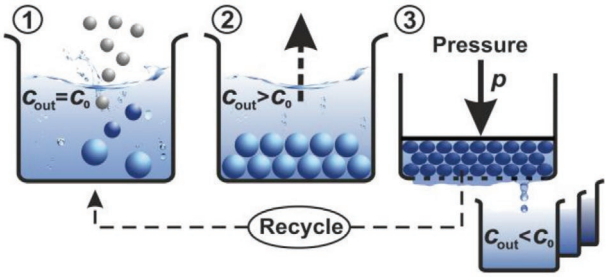

Scheme 1. Basic principle of the desalination process. The salinity of the external solution is reduced in a three-step process. 1) Mixing of dry polyelectrolyte hydrogel particles with the saline external solution. 2) The supernatant phase is salt enriched due to the salt rejection and removed. 3) Recovery of salt depleted water by lowering the piston and applying an external pressure while the outflow is continuously collected in 3–10 mL fractions.

(G'') moduli were taken at a frequency of ω = 6.3 rad s^{-1} (f = 1 Hz) to compare the rheological behavior of different hydrogel samples. The error bars in the respective graphs show the standard deviation around the mean value.

2.5. Salt Rejection Measurements

The salt partitioning between the gel phase and the external solution was analyzed via salt rejection measurements in a 1 wt% NaCl (0.171 mol L^{-1}) solution. The dried hydrogel samples were mixed overnight with the sodium chloride solution (total mass of the mixture m_{total} = 40 g) in a specific ratio Q_{rel} = m_s/m_{absorb} = 2, where m_s refers to the mass of the brine solution and m_{absorb} to the maximum water uptake according to Q_{eq}. The fixing of the parameter Q_{rel} = 2 ensures that one half of the brine volume is located in the swollen hydrogel and the other half in the supernatant phase, as depicted in the second step of **Scheme 1**. The salt concentration of the supernatant phase was analyzed by conductivity measurements (SevenMulti, Mettler Toledo, Gießen, Germany) upon an appropriate calibration.[9] The ratio of the salt concentration in the supernatant phase, c_{out}, to the initial concentration, c_0, defines the salt rejection (SR)

$$SR = c_{out} / c_0 \times 100\% \tag{5}$$

2.6. Desalination Experiment

The desalination of seawater was conducted on a custom-built hydraulic press setup, as illustrated in Figure 1. The apparatus consists of a press chamber with a total volume of 400 mL and a piston that transfers the pressure to the sample, while a sieve unit (3–5 µm pore size) holds back the hydrogel particles. A detailed description of the construction is found in previous work.[9] During the compression of the particles the pressure inside the chamber and the volume flux is measured by a pressure sensor (SD-40, Suchy Messtechnik, Lichtenau, Germany) and a distance gauge (MarCator 1086, Mahr, Göttingen, Germany), respectively. In the first step of the experiment, dry hydrogel particles were swollen overnight in artificial seawater with a concentration of c_{sea} = 0.171 mol L^{-1} (11.6 g L^{-1}) that resembles the concentration of 1 wt% NaCl solution c_{NaCl} = 0.171 mol L^{-1} (10 g L^{-1}). The mass ratio of seawater to swollen hydrogel was kept constant (Q_{rel} = 2), as described in the salt rejection measurement and in previous work.[23] The mixture is transferred into the press chamber and the supernatant phase is removed by applying a small pressure (1 bar). The sample is then compressed with an increasing pressure of 1 bar min^{-1} to a maximum pressure of 80 bar to ensure a constant volume flux. The emerging water was continuously collected in fractions and the ion content measured offline by inductively coupled plasma optical emission spectroscopy (ICP-OES) and ion chromatography (IC) for cations and anions, respectively (see the Supporting Information for more details). The expended energy E of the desalination process was calculated by the numerical integration of the pressure–volume work according to Equation (6)

$$E_i = -\int_{i=0}^{n} p_i \times \mathrm{d}V_i \tag{6}$$

while the removed salt mass Δm (salt) is calculated by Equation (7)

$$\Delta m\,(\mathrm{salt}) = m\,(\mathrm{salt, initial}) - m\,(\mathrm{salt, fractions}) = c_0 \sum_i V_i - \sum_i (c_i \times V_i) \tag{7}$$

where V_i is the volume of fraction i. Subsequently, the ratio of the expended energy E to removed salt mass Δm (salt) was defined as the parameter κ, which is used to quantify the energy demand of the desalination and calculate the specific energy E_{m^3} to remove 35 kg of salt in one cubic meter seawater by Equations (8) and (9)

$$\kappa = \frac{E}{\Delta m(\mathrm{NaCl})}\,[\mathrm{kWs\,g^{-1}}] \tag{8}$$

$$E_{m^3} = \kappa \times \frac{35\,000\ \mathrm{g}}{3600\ \mathrm{s\,h^{-1}}} \approx 10 \times \kappa\,[\mathrm{kWh\,m^{-3}}] \tag{9}$$

A detailed description of the calculation can be found in previous studies.[22,23] In total, the basic principle of the desalination follows a three-step process, as displayed in Scheme 1.

3. Results and Discussion

3.1. Swelling Behavior

During the desalination process salt depleted water is recovered by deswelling the particles (see Scheme 1), hence the hydrogel must exhibit a certain minimum degree of swelling at equilibrium (Q_{eq} > 10 g g^{-1}) in seawater to obtain a reasonable outflow. Water absorbency measurements are conducted for anionic

© 2020 The Authors. Published by Wiley-VCH GmbH

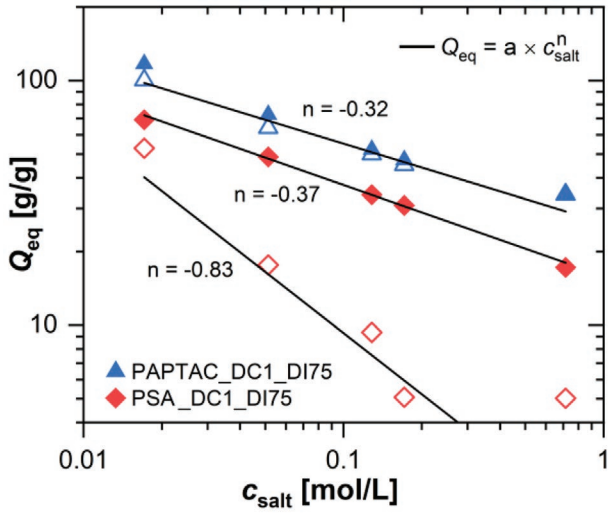

Figure 2. Degree of swelling at equilibrium (Q_{eq}) in different sodium chloride (solid symbols) and artificial seawater (open symbols) salt concentrations (c_{salt}) of an anionic PSA (diamonds) and cationic PAPTAC (triangles) hydrogel. Both hydrogels have a degree of crosslinking of DC = 1 mol% and degree of ionization of DI = 75 mol%. A general equation $Q_{eq} = a \times c_{salt}^{n}$ is used for a power law relationship, resembling the reduction of the Debye length ($\lambda_D \sim c_{salt}^{-1/2}$).

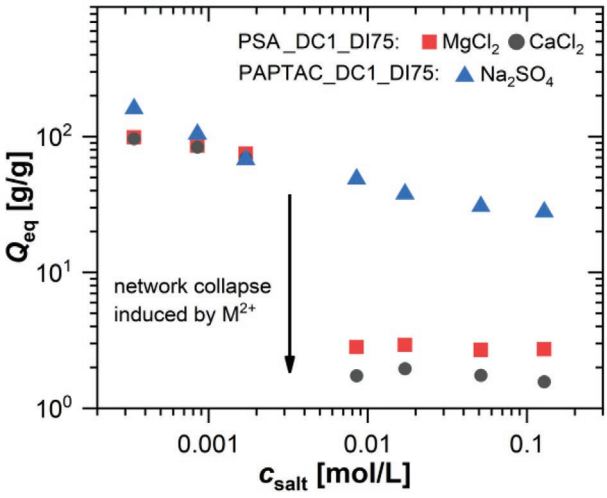

Figure 3. Influence of multivalent salt solutions ($MgCl_2$, $CaCl_2$, and Na_2SO_4) at different concentrations on the degree of swelling at equilibrium (Q_{eq}) of cationic PAPTAC (triangles in Na_2SO_4) and anionic PSA (squares in $MgCl_2$ and circles in $CaCl_2$) hydrogels with equivalent DC (1 mol%) and DI (75 mol%). A substantial collapse by a factor of 25 at 0.003 mol L^{-1} in Mg^{2+} and Ca^{2+} solutions is found. This phenomenon is not observed for divalent SO_4^{2-} anions.

PSA and cationic PAPTAC hydrogels to compare the swelling behavior as the function of the artificial seawater concentration c_{sea}, as shown in **Figure 2**.

The Q_{eq} values decrease monotonically with higher salt concentrations due to the reduction of the difference in the osmotic pressure between hydrogel and the external solution.[20] The obtained values for Q_{eq} are fitted by a power law following the general equation, $Q_{eq} = a \times c_{salt}^{n}$, which refers to the screening of charges along the polymer backbone according to the reduction of the Debye length, $\lambda_D \sim c_{salt}^{-1/2}$.[30,31] As a result, the electrostatic repulsion between monomer units is reduced and consequently Q_{eq} decreases. However, lower values for the exponent are also found. The power law is valid for weakly crosslinked polyelectrolyte chains and values for the exponent $n < -0.5$ are expected to arise with increasing DC due to the restricted motion of the chains.[23] In contrast to the cationic hydrogel with $n = -0.32$ in seawater, a distinct deviation for the anionic hydrogel with a sharp decrease of Q_{eq} in seawater with $n = -0.83$ is observed. This decrease in seawater is more than two times higher than in sodium chloride solutions. Seawater contains multivalent ions, such as Mg^{2+}, Ca^{2+} and SO_4^{2-}. During the swelling process the sodium counterions of the anionic carboxylate groups are exchanged with Mg^{2+} and Ca^{2+} ions which induce a reduction of the swelling capacity through ionic interactions with the polymer backbone.[26,32] The cationic hydrogel, however, shows a strong salt resistance toward seawater and exhibits similar values for Q_{eq} as in sodium chloride solution. Moreover, this result suggests that divalent sulfate anions are not affecting the swelling capabilities of the cationic PAPTAC hydrogel. To further verify the salt resistant behavior of cationic PAPTAC toward divalent sulfate ions, the water absorbency is measured in pure Na_2SO_4 salt solution. As a comparison the water absorbency of anionic PSA hydrogels is measured in $MgCl_2$ and $CaCl_2$ solutions, as depicted in **Figure 3**.

In pure Mg^{2+} and Ca^{2+} solutions, the anionic PSA hydrogel exhibits a strong salt sensitivity in the degree of swelling. Consequently, at low salt concentrations ($c_{salt} < 0.01$ mol L^{-1}) a sharp volume transition is found where Q_{eq} is decreased approximately by a factor of 25. At this concentration a three times higher value is found in seawater, as shown in Figure 2. This deviation from seawater shows that the influence of multivalent ions depends on the ratio of salts in the external solution, as monovalent ions and divalent ions compete for the negatively charged carboxylate groups.[27,30,31,33] In contrast, an interaction of cationic hydrogels with divalent SO_4^{2-} anions is not observed. Hence, utilizing APTAC as a charged monomer with a quaternary amine functional group ($-N^+Me_3$) for the introduction of positive charges in the polymer backbone facilitates a resistance of Q_{eq} toward multivalent ions that are present in seawater.

To study the influence of synthetic parameters on the hydrogel swelling behavior, water absorbency measurements are performed for different PAPTAC compositions with varying DC and DI, as displayed in **Figure 4**.

The swelling behavior of the cationic hydrogels in NaCl solution and seawater shows similar values, which further indicates that the degree of swelling is mainly influenced by the synthesis parameters and is not altered by additional salts that are present in seawater. The Q_{eq} decreases with higher DC which influences the average molecular weight, $\bar{M}_c$, between two adjacent crosslinking points. Therefore, at lower DC a looser network with longer elastic chains and higher absorption capacity is formed.[34,35] For large swelling ratios ($Q_{eq} > 10$ g g^{-1}) this

© 2020 The Authors. Published by Wiley-VCH GmbH

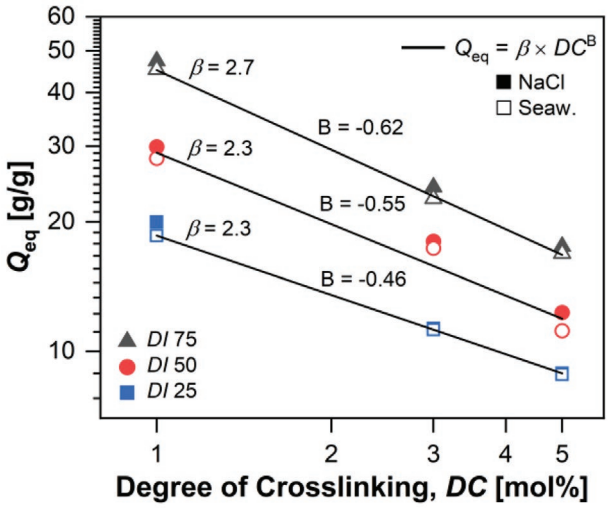

Figure 4. Degree of swelling at equilibrium (Q_{eq}) for PAPTAC hydrogels with varying degree of ionization (DI) is plotted as the function of the degree of crosslinking (DC). The degree of swelling is measured in artificial seawater (solid symbols) and sodium chloride solution (open symbols) with a concentration of c = 0.171 mol L^{-1}. The obtained values in seawater are fitted with the equation $Q_{eq} = \beta \times DC^B$ following a power law.

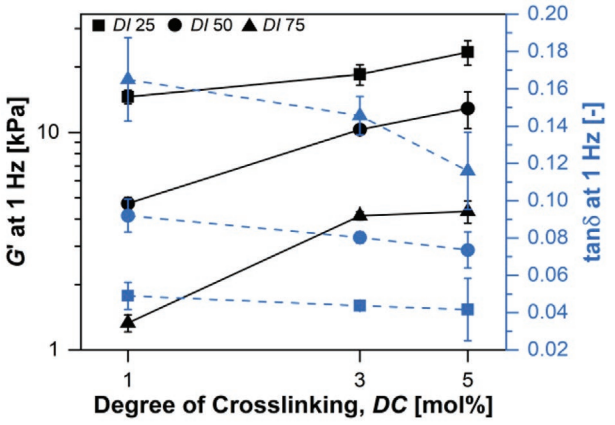

Figure 5. Rheological studies of cationic PAPTAC hydrogels with varying degree of crosslinking (DC) and degree of ionization (DI). The values for the elastic modulus (G') and loss tangent, tan δ, were taken at a strain of γ_0 = 0.1% in the linear regime with a frequency of ω = 6.3 rad s^{-1} (f = 1 Hz). The lines are guide to the eye.

dependency can be approximated by a scaling law according to the Flory–Rehner equation

$$Q_{eq} = \left[\frac{\bar{v}\left(1/2 - 2\chi_{12}\right)\bar{M}_c}{V_1} \right]^{3/5} = \beta(\bar{M}_c)^{3/5} \quad (10)$$

where β is a constant related to the specific volume of the polymer $\bar{v}$, the molar volume of water V_1, and the Flory polymer–water interaction parameter χ_{12}.[36,37] The average molecular weight between crosslinking points is proportional to the degree of crosslinking, $\bar{M}_c \sim DC^{-1}$. Accordingly, the PAPTAC hydrogels follow this scaling law with exponents ranging from –0.46 to –0.62 decreasing with higher DI values. To explain the dependency on DI, two effects have to be considered. Primarily, DI determines the amount of positive charges in the polymer backbone. At higher DI the osmotic potential of the hydrogel is increased, and thus higher Q_{eq} are observed. In addition, DI refers to the molar fraction of the positive charged monomer APTAC in the hydrogel composition and with increasing DI lesser amounts of AM are present. It is known that the use of AM as a copolymer increases the mechanical properties and stiffness of polyelectrolyte hydrogels.[38,39] Thus, at lower DI the highest strengthening effects and lower Q_{eq} values are expected which is in agreement with the water absorbency measurements.

3.2. Rheological Investigation

To further study the effect of the initial hydrogel composition on the mechanical properties, oscillatory shear measurements are performed.[40,41] Frequency sweeps for all hydrogel samples show that the elastic modulus (G') is constant over the whole frequency range (0.1–100 Hz) while exceeding the loss modulus (G'') by a factor of 10 which confirms network formation throughout the whole sample range (see Figure S1 in the Supporting Information). Values for G' range from 1.5 to 24 kPa and increase with higher DC. However, a distinct deviation of G' for different DI is observed, as shown in **Figure 5**.

As predicted by the rubber elasticity theory, G' increases as a function of DC.[36,42,43] With increasing concentration of the crosslinking agent, more but shorter elastic chains are introduced into the network, exerting higher elastic forces during deformation. Additionally, G' increases with decreasing DI, indicating that the hydrogels become more rigid as the concentration of AM rises in the initial composition. The highest values for G' are found for hydrogel compositions with high amounts of AM (DI = 25 mol%), which exceed samples with low amounts (DI = 75 mol%) by a factor of at least 5 at equivalent DC. This deviation indicates that the initial monomer composition distinctly influences the mechanical properties and is further demonstrated in the values of tan δ that is used as a measure to quantify the extent of viscous contributions in the material (tan $\delta = G''/G'$). With increasing DC, tan δ decreases in a linear fashion for high DI (75 mol%) and is constant for lower DI values. Note that the hydrogel samples are analyzed in the as-prepared state without purification. Hence, unreacted moieties and non-crosslinked chains (sol) are present during the measurement. Increased tan δ values and lower elastic moduli (G') further indicate that the crosslinking efficiency is reduced as the concentration of APTAC increases in the reaction mixture. The presence of enhanced electrostatic repulsion effects between APTAC monomer units and the propagating polymer chains as well as the repulsion of neighboring polymer chains during network formation may explain a reduction in the crosslinking efficiency.[38,39]

© 2020 The Authors. Published by Wiley-VCH GmbH

3.3. Salt Rejection Measurements

Utilizing polyelectrolyte hydrogels as a separation medium for desalination involves two mechanisms or stages. First, the dry hydrogel particles absorb water due to the hydrophilicity and the difference in the osmotic pressure. Then, according to the Donnan theory the fixed charges and counterions in the polymer backbone hinder mobile salt ions from further entering the hydrogel network and establishing an equal concentration inside the gel phase and the surrounding solution.[44] Therefore, the concentration of mobile salts inside the gel is lower compared to the external solution as there are additional charge contributions from the network. This distribution of mobile salts between the gel phase and supernatant phase is referred to as salt partitioning.[45] Consequently, the combination of both effects, water absorption and the salt partitioning, leads to a salt enrichment in the supernatant phase. The ratio of the concentration in the supernatant phase (c_{supern}) to the initial salt concentration (c_0) can be further defined as salt rejection (SR), see Equation (5). As discussed in previous work,[9,22] the efficiency criterion for the desalination considers the energy expended during compression of the hydrogel particles as well as the amount of removed salt according to Equations (8) and (9). Hence, the extent of the salt partitioning is a crucial quantity for the desalination efficiency, and SR measurements can be utilized as a rather easily accessible tool for the estimation of the desalination efficiency in the press setup.

The SR is a function of the fixed charge concentration, and thus highly depends on Q_{eq}. At higher Q_{eq} values, more water is absorbed and SR decreases. By plotting SR as the function of the fixed charge concentrations, the obtained values can be compared to the Donnan theory as shown in Equation (11)[9,23]

$$SR_{Donnan} = \left(1 - \frac{2 \times c_0}{\left(\frac{f_{eff} \times c_+}{2}\right) + 2 \times c_0}\right) \quad (11)$$

where c_0 is the initial concentration of the external solution and c_+ is the concentration of APTAC monomer units (fixed positive charges) inside the hydrogel according to DI and the parameter f_{eff} resembles the effective charge fraction with values ranging from $f_{eff} = 0$ to 1. The experimental data obtained for SR is plotted as the function of Q_{eq} and c_+, as depicted in **Figure 6**.

Considering the simplicity of the Donnan model, the experimentally obtained SR values can be described as the function of the charge density using approximately an effective charge fraction of $f_{eff} = 0.4$. Correspondingly, high SR values up to 17 mol% are achieved at low Q_{eq} values as less water is absorbed. Multiple sources attribute to the deviation from the ideal Donnan theory. Previous studies showed that the Donnan theory fails to describe quantitatively the salt partitioning of highly charged hydrogels as the salt rejection is overpredicted.[9,45] Additionally, the effective charge density along the polymer backbone may be reduced by the so called Manning condensation, which occurs when the distance between two neighboring charged monomer units is lower than the Bjerrum length ($l_{Bjerrum} = 0.7$ nm in water).[46] At this critical threshold counterions condense on the polyelectrolyte, limiting the effective charge density. In the herein presented cationic hydrogel system, the distance between positive charges is expected to be larger than the Bjerrum length, since six chemical bonds in the APTAC side group separate the positive charges of the quaternary amine moieties from the polymer backbone. However, the theory of Manning describes an idealized linear charged chain of zero radius and does not take into account any molecular properties of polyelectrolyte chains, for instance the stiffness and restricted rotation of the amide bonds. Hence, deviations from the theory are expected especially at highly crosslinked hydrogels, which additionally contribute to the reduction of the charge density. Furthermore, the APTAC concentration, and thus the concentration of fixed positive charges is calculated from the mass fraction of polymer. We estimate the content of APTAC from the initial hydrogel composition obtained by the DI. The highest value for SR is found for the sample with

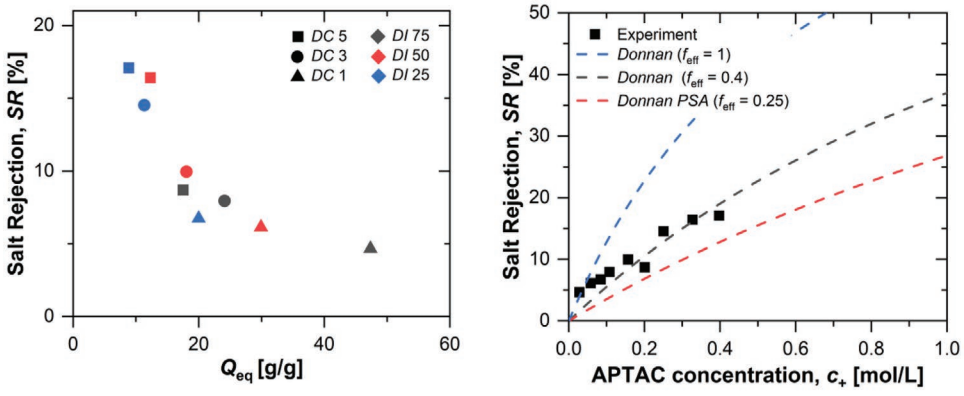

Figure 6. Salt rejection (SR) which is measured in 0.171 mol L^{-1} NaCl solution for PAPTAC hydrogel with varying degree of crosslinking (DC) and degree of ionization (DI) is plotted as the function of the degree of swelling at equilibrium (Q_{eq}) (left) and the concentration of APTAC monomer (positive charges, c_+) inside the swollen hydrogel (right). The experimental data is compared to the Donnan model according to Equation (11) with effective charge fractions of $f_{eff} = 1$, 0.4, and 0.25. The latter was obtained in a previous study for poly(sodium acrylate) hydrogels and is used for comparison.[23]

© 2020 The Authors. Published by Wiley-VCH GmbH

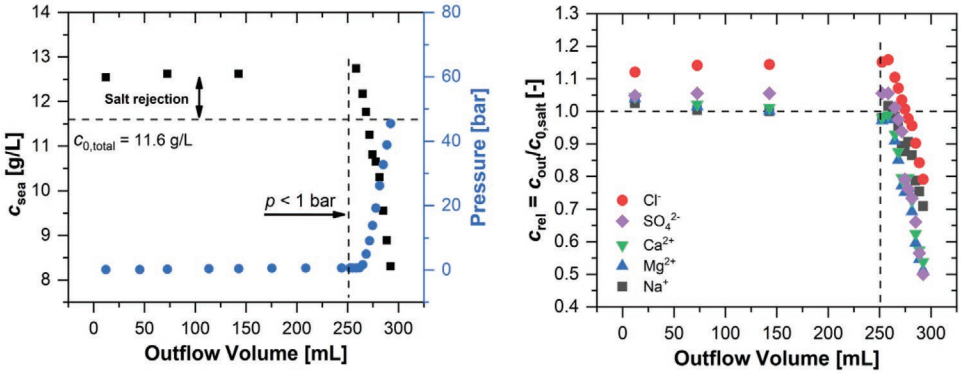

Figure 7. Left: Desalination of seawater ($c_{0,total}$ = 0.171 mol L^{-1}, 11.6 g L^{-1}) with the custom-built press setup in a three-step process using cationic PAPTAC hydrogel particles with DC = 5 mol% and DI = 25 mol% as separation medium. An external pressure (p < 1 bar) by lowering the piston is applied to remove the salt enriched supernatant phase where $c_{sea} > c_{0,total}$. Thereafter, the pressure is linearly increased (1 bar min^{-1}) to deswell the particles and recover salt depleted water. The outflow is collected continuously in 3–10 mL fractions and subsequently their ion content measured. Right: Relative concentration ($c_{rel} = c_{out}/c_{0,salt}$) of mobile ions shows the salt partitioning between the gel phase and the external solution during the desalination experiment.

DC = 5 mol% and DI = 25 mol%, which exhibits the highest APTAC concentration and the lowest Q_{eq}. Maximizing SR is crucial to optimize the desalination efficiency. Therefore, it is required to synthesize highly charged hydrogels while maintaining low degrees of swelling to increase the fixed charge concentration.

3.4. Desalination Experiments

As a proof of concept, the sample with the highest SR (DC = 5 mol%; DI = 25 mol%) is chosen for the desalination of artificial seawater with a concentration similar to 1 wt% NaCl solution, c_{sea} = 0.171 mol L^{-1} (11.26 g L^{-1}) in the demonstrated press setup (see Figure 1). The results of the desalination process are displayed in **Figure 7**.

The concentration of the outflow (c_{out}) decreases linearly with a rate of dc_{out}/dV = –0.13 g ml L^{-1} as the pressure is increased to deswell the particles, as displayed in Figure 7 (left). A salt reduction of 40% compared to the initial concentration is achieved at the last fraction. The energy demand for the desalination experiment is calculated from the pressure and elution volume by means of the volume work where the numerical integration of the p–V curve gives the expended energy E.[22,23] The energy demand for the desalination of seawater with a concentration of 11.6 g L^{-1} is estimated according to Equation (9) to E_{m^3} = 17.6 kWh m^{-3}.

Additionally, a distinct difference of the salt partitioning for different ions is found, as shown in Figure 7 (right). While a strong salt rejection is observed for chloride ions ($c_{rel}(Cl^-) = c_{out}/c_0 = 1.1$), the salt rejection for divalent sulfate ions is slightly lower ($c_{rel}(SO_4^{2-}) = 1.05$). The counterion for the cationic APTAC monomer during synthesis is chloride with a concentration of $c_{Cl,syn}$ = 0.277 mol L^{-1}. The chloride concentration inside the gel is therefore already high, prior to the desalination experiment, and thus the concentration gradient from the external solution toward the inside of the hydrogel is weaker compared to sulfate anions. The tendency to diffuse into the hydrogel is stronger for sulfate ions. As a result of the diffusion, two chloride ions are exchanged with sulfate to maintain electroneutrality which further enhances the salt rejection of chloride. A distinct salt rejection for the cations is not observed and the cations distribute evenly between the gel and the supernatant phase. However, as shown in the water absorbency measurements the multivalent ions do not influence the swelling behavior of the synthesized cationic hydrogels which makes them suitable as separation medium in multivalent ion rich solutions. In contrast, PSA hydrogels show a network collapse in the presence of multivalent cations, fully preventing the desalination of seawater. Hence, our emphasis in future studies is to extend the application of cationic hydrogels as separation medium while optimizing the desalination efficiency, for instance, by decoupling the charge density from mechanical properties.

4. Conclusion

In this study, a series of cationic poly(acrylamide-*co*-(3-acrylamidopropyl)trimethylammonium chloride) hydrogels with varying DC and DI are synthesized for the application as separation medium in the desalination of seawater. The swelling behavior is studied in sodium chloride solution and artificial seawater while comparing it to an anionic PSA reference system. By studying the swelling behavior, we found that the cationic hydrogels are resistant toward the seawater composition that contains multivalent ions, such as Mg^{2+}, Ca^{2+}, and SO_4^{2-}, whereas a strong decrease of the swelling capacity is observed for the anionic hydrogel. Artificial seawater with a concentration of 11.6 g L^{-1} was desalinated with a custom-built press setup in a three-step process utilizing cationic hydrogel particles as separation medium. The energy demand of the desalination approach was estimated to E_{m^3} = 17.6 kWh m^{-3} with a total reduction of the salt concentration by up to 40%. To further increase the efficiency of the process, the charge density of the hydrogel particles has to be maximized while simultaneously maintaining reasonable degrees of swelling (Q_{eq} > 10 g g^{-1}) to allow a sufficient outflow

© 2020 The Authors. Published by Wiley-VCH GmbH

of salt depleted water. Moreover, the mechanical moduli have to be minimized to reduce the energy demand for deswelling the particles. This decoupling of the mechanical strength from the charge density is the aim of our next studies. Furthermore, we want to investigate blocking phenomena related to biofouling and clogging that drastically reduce the membrane efficiency of the reverse osmosis processes. Since the particles in the here proposed technique exhibit alternating swelling and deswelling cycles, a backwashing and self-cleaning effect could achieve a reduction of blocking phenomena.

Supporting Information

Supporting Information is available from the Wiley Online Library or from the author.

Acknowledgements

The authors greatly acknowledge financial support from the "Sonderforschungsbereich 1176" (project C1) funded by the German Research Council (DFG) and the Fonds der Chemischen Industrie (VCI). Furthermore, the authors wish to thank Prof. Horn (Engler-Bunte-Institut, KIT) for measurements of the ionic content.

Open access funding enabled and organized by Projekt DEAL.

Conflict of Interest

The authors declare no conflict of interest.

Keywords

hydrogels, membranes, polyelectrolytes, rheology, swelling

Received: June 16, 2020
Revised: July 24, 2020
Published online: August 16, 2020

[1] C. J. Vörösmarty, P. B. McIntyre, M. O. Gessner, D. Dudgeon, A. Prusevich, P. Green, S. Glidden, S. E. Bunn, C. A. Sullivan, C. R. Liermann, P. M. Davies, *Nature* **2010**, *467*, 555.
[2] J. Kucera, *Desalination: Water from Water*, Wiley Online Library, Salem, MA, **2014**.
[3] E. Jones, M. Qadir, M. T. van Vliet, V. Smakhtin, S.-M. Kang, *Sci. Total Environ.* **2019**, *657*, 1343.
[4] M. Elimelech, W. A. Phillip, *Science* **2011**, *333*, 712.
[5] N. M. Wade, *Desalination* **2001**, *136*, 3.
[6] S. A. Avlonitis, K. Kouroumbas, N. Vlachakis, *Desalination* **2003**, *157*, 151.
[7] S. A. Avlonitis, *Desalination* **2002**, *142*, 295.
[8] J. Höpfner, C. Klein, M. Wilhelm, *Macromol. Rapid Commun.* **2010**, *31*, 1337.
[9] J. Höpfner, T. Richter, P. Košovan, C. Holm, M. Wilhelm, *Prog. Colloid Polym. Sci.* **2013**, *140*, 247.
[10] F. L. Buchholz, A. T. Graham, *Modern Superabsorbent Polymer Technology*, Wiley-VCH, New York **1998**.
[11] X. Guo, S. Theissen, J. Claussen, V. Hildebrand, J. Kamphus, M. Wilhelm, B. Luy, G. Guthausen, *Macromol. Chem. Phys.* **2018**, *219*, 1800100.
[12] X. Guo, C. Pfeifer, M. Wilhelm, B. Luy, G. Guthausen, *Macromol. Chem. Phys.* **2019**, *220*, 1800525.
[13] M. J. Zohuriaan-Mehr, H. Omidian, S. Doroudiani, K. Kabiri, *J. Mater. Sci.* **2010**, *45*, 5711.
[14] S. Ganta, H. Devalapally, A. Shahiwala, M. Amiji, *J. Controlled Release* **2008**, *126*, 187.
[15] K. S. Kazanskii, S. A. Dubrovskii, *Polyelectrolytes Hydrogels Chromatographic Materials*, Springer, Berlin **1992**, pp. 97–133.
[16] D. DeRossi, K. Kajiwara, Y. Osada, A. Yamauchi, *Polymer Gels: Fundamentals and Biomedical Applications*, Plenum Press, New York **1991**.
[17] L. Arens, F. Weißenfeld, C. O. Klein, K. Schlag, M. Wilhelm, *Adv. Sci.* **2017**, *4*, 1700112.
[18] A. Jangizehi, C. Fengler, L. Arens, M. Wilhelm, *Macromol. Mater. Eng.* **2020**, 2000174.
[19] T. Y. Cath, A. E. Childress, M. Elimelech, *J. Membr. Sci.* **2006**, *281*, 70.
[20] A. Katchalsky, I. Michaeli, *J. Polym. Sci.* **1955**, *15*, 69.
[21] J. Ricka, T. Tanaka, *Macromolecules* **1984**, *17*, 2916.
[22] L. Arens, J. B. Albrecht, J. Höpfner, K. Schlag, A. Habicht, S. Seiffert, M. Wilhelm, *Macromol. Chem. Phys.* **2017**, *218*, 1700237.
[23] L. Arens, D. Barther, J. Landsgesell, C. Holm, M. Wilhelm, *Soft Matter.* **2019**, *15*, 9949.
[24] W. Ali, B. Gebert, T. Hennecke, K. Graf, M. Ulbricht, J. S. Gutmann, *ACS Appl. Mater. Interfaces* **2015**, *7*, 15696.
[25] T. Richter, J. Landsgesell, P. Košovan, C. Holm, *Desalination* **2017**, *414*, 28.
[26] I. Ohmine, T. Tanaka, *J. Chem. Phys.* **1982**, *77*, 5725.
[27] F. Horkay, I. Tasaki, P. J. Basser, *Biomacromolecules* **2001**, *2*, 195.
[28] M. A. Barakat, N. Sahiner, *J. Environ. Manage* **2008**, *88*, 955.
[29] ASTM Standard D1141-98. *Standard Practice for the Preparation of Substitute Ocean Water*, ASTM, West Conshohocken **2013**.
[30] F. Horkay, I. Tasaki, P. J. Basser, *Biomacromolecules* **2000**, *1*, 84.
[31] M. Mussel, P. J. Basser, F. Horkay, S. Matter **2019**, *15*, 4153.
[32] E. Vasheghani-Farahani, J. H. Vera, D. G. Cooper, M. E. Weber, *Ind. Eng. Chem. Res.* **1990**, *29*, 554.
[33] F. Horkay, A. M. Hecht, C. Rochas, P. J. Basser, E. Geissler, *J. Chem. Phys.* **2006**, *125*, 234904.
[34] J. Höpfner, G. Guthausen, K. Saalwächter, M. Wilhelm, *Macromolecules* **2014**, *47*, 4251.
[35] F. Cavalli, C. Pfeifer, L. Arens, L. Barner, M. Wilhelm, *Macromol. Chem. Phys.* **2020**, *221*, 1900387.
[36] P. J. Flory, J. Rehner, *J. Chem. Phys.* **1943**, *11*, 512.
[37] C.-C. Lin, A. T. Metters, *Adv. Drug Delivery Rev.* **2006**, *58*, 1379.
[38] B. A. Baker, R. L. Murff, V. T. Milam, *Polymer* **2010**, *51*, 2207.
[39] J. L. Trompette, E. Fabrègue, G. Cassanas, *J. Polym. Sci., Part B: Polym. Phys.* **1997**, *35*, 2535.
[40] G. M. Kavanagh, S. B. Ross-Murphy, *Prog. Polym. Sci.* **1998**, *23*, 533.
[41] J. M. Zuidema, C. J. Rivet, R. J. Gilbert, F. A. Morrison, *J. Biomed. Mater. Res., Part B* **2014**, *102*, 1063.
[42] W. Oppermann, S. Rose, G. Rehage, *Br. Polym. J.* **1985**, *17*, 175.
[43] M. L. Oyen, *Int. Mater. Rev.* **2014**, *59*, 44.
[44] A. Philipse, A. Vrij, *J. Phys.: Condens. Matter* **2011**, *23*, 194106.
[45] P. Košovan, T. Richter, C. Holm, *Macromolecules* **2015**, *48*, 7698.
[46] G. S. Manning, *J. Chem. Phys.* **1969**, *51*, 924.

© 2020 The Authors. Published by Wiley-VCH GmbH